Curcumin Ameliorates AATF-mediated Liver Damage and Inflammation to Cancer in NASH-HCC

Akshatha N. Srinivas[1*], Diwakar Suresh[1*], Saravana Babu Chidambaram[2], Prasanna K. Santhekadur[1], and Divya P. Kumar [1**]

[1]Department of Biochemistry, CEMR lab, JSS Medical College, JSS Academy of Higher Education and Research, Mysuru, Karnataka, India

[2]Department of Pharmacology, JSS College of Pharmacy, JSS Academy of Higher Education and Research, Mysuru, Karnataka, India

*These authors share co-first authorship.

[**]**Correspondence:**
Dr. Divya P. Kumar
Assistant Professor
Department of Biochemistry
CEMR, JSS Medical College
JSS Academy of Higher Education and Research
SS Nagar, Mysuru, India-570015
Email: divyapk243@gmail.com/
divyapkumar@jssuni.edu.in

Abstract

In tandem with the expanding obesity pandemic, the prevalence of nonalcoholic steatohepatitis (NASH)-associated hepatocellular carcinoma (HCC) is predicted to rise globally, creating a significant need for therapeutic agents to treat the disease. In this study, we aim to examine the hepatoprotective effect of curcumin and elucidate the mechanism by which curcumin ameliorates NASH and prevents tumorigenesis. A preclinical murine model that recapitulates human NASH-HCC in which mice were exposed to a very low dose of carbon tetrachloride (CCl_4- 0.2 μl/g) once per week with administration of chow diet and normal water (CDNW) or high-fat western diet and ad lib sugar water (WDSW) was used. Compared to mice on WDSW/CCl_4 and vehicle controls, mice receiving WDSW/CCl_4 and curcumin showed significant reductions in liver enzymes and dyslipidemia and ameliorated steatosis, lobular inflammation, and hepatocellular ballooning in WDSW/CCl_4 mice. In addition, curcumin treatment markedly reduced the hepatic expression of inflammatory markers, fibrogenic genes, and oncogenic markers. Interestingly, curcumin inhibited apoptosis antagonizing transcription factor (AATF), an oncogene overexpressed in NASH-HCC. Furthermore, the anti-tumor effects of curcumin via AATF were validated using human HCC cells. Kruppel-like factor 4 (KLF4) was significantly upregulated by curcumin in NASH liver and HCC cells. Curcumin treatment effectively inhibited the progression of NASH to HCC by downregulating the expression of AATF via the KLF4-Sp1 (specificity protein-1) signaling pathway. Herein, we report the novel molecular link between curcumin and AATF in reducing hepatocarcinogenesis, and these preclinical data provide a strong rationale for developing curcumin for the treatment of NASH-HCC in humans.

Keywords

Curcumin, nonalcoholic steatohepatitis, hepatocellular carcinoma, apoptosis antagonizing transcription factor, inflammation, tumorigenesis

Abbreviations

HCC, hepatocellular carcinoma; NAFLD, nonalcoholic fatty liver disease; NASH, nonalcoholic steatohepatitis; AATF, apoptosis antagonizing transcription factor; STAT3, signal transducer and activator of transcription 3; TNF-α, tumor necrosis factor- α; ER, endoplasmic reticulum; NF-κB, nuclear factor kappa B; KLF4, kruppel-like factor 4; Sp1, specificity protein 1; CDNW, chow diet normal water; WDSW, western diet sugar water; CCl_4, carbon tetrachloride; VC, vehicle control; ALT, alanine transaminase; AST, aspartate transaminase; IL-1β, interleukin-1β; IL-6, interleukin-6; ERK1/2, extracellular signal-regulated protein kinase; JNK, Jun N-terminal kinase; CD31, cluster of differentiation 31; AFP, alpha-fetoprotein.

1. Introduction

Hepatocellular carcinoma (HCC), a highly aggressive type of liver cancer known to develop in the setting of chronic liver disease, is a serious health care challenge worldwide [1]. There is mounting evidence that the etiologies of HCC are rapidly shifting towards obesity and the metabolic syndrome [2]. Given the 25% global prevalence of nonalcoholic fatty liver disease (NAFLD), a hepatic manifestation of metabolic syndrome, NAFLD-related HCC is an emerging cause of liver tumorigenesis [3,4]. A progressive form of non-alcoholic fatty liver disease (NAFLD), non-alcoholic steatohepatitis (NASH), raises the risk of cirrhosis and HCC. The exact mechanisms by which NASH leads to HCC are not fully understood, but it is believed that chronic inflammation and cellular damage caused by NASH accelerate fibrogenesis and create an environment that is more conducive to cancerous cell growth and development [5]. NASH-associated HCC is often associated with poor survival due to several factors, including poor prognosis, late diagnosis, and inadequate management. Unlike other types of HCC, NASH-HCC can develop even in the absence of cirrhosis, making it more difficult to detect and manage [6]. The complexities and heterogeneity of the NASH-HCC pathophysiology have hampered treatment strategies. Multifactorial processes, including genetic, metabolic, immunogenic, and endocrine mechanisms, contribute to the transition of damaged hepatocytes into HCC [7,8,9]. At a cellular level, genetic and epigenetic events orchestrate the pro-oncogenic milieu against a background of insulin resistance and inflammation [10,11]. Thus, a mechanistic approach to studying the root cause of NASH-HCC and the development of therapeutic strategies for NASH-HCC is the need of the hour.

Apoptosis antagonizing transcription factor (AATF) is a multifunctional protein known to play a critical role in key cellular processes [12]. AATF is an emerging modulator of cell proliferation, survival, and apoptosis depending on the cellular status, thereby serving as both a prooncogene and a tumor suppressor gene [13-15]. Studies have shown the involvement of the AATF in many cancers, such as leukemia, breast cancer, neuroblastoma, lung cancer, and colon cancer [16-20]. Investigations by Kumar et al., have shown elevated levels of AATF in human and mouse NASH-HCC [21]. In a diet-induced animal model of NAFLD (DIAMOND), AATF contributes to tumorigenesis via STAT3-dependent activation of monocyte chemoattractant protein-1 (MCP-1) [21] . AATF is also known to significantly contribute to various hallmarks of HCC, and we have recently elucidated the regulatory role of AATF in HCC angiogenesis [22].

Natural monomeric products are extensively studied for their hepatoprotective and anti-inflammatory efficacy, which can improve NASH [23]. Curcumin, an active component of curcuminoids derived from the rhizome of turmeric (Curcuma longa, Zingiberaceae), is a diarylheptane and is known for its anti-inflammatory, antioxidant, and anti-cancer properties [24-26]. Curcumin is known to mediate anticancer effects by modulating inflammatory cytokines, growth factors, transcription factors, and multiple signaling proteins [27]. Several studies have shown the positive effects of curcumin on ameliorating NASH. Curcumin lowers de novo lipogenesis by reducing the levels of sterol regulatory element binding protein 1-c (SREBP-1c) and adipose differentiation-related protein (ADRP) [28]. Further, tumor necrosis factor- α (TNF-α) and reactive oxygen species (ROS) levels were also found to be reduced upon

curcumin treatment in HFD-induced NASH [29]. In the streptozotocin (STZ)-induced NASH-HCC model, curcumin protected liver damage from ER stress and related inflammation by inhibiting the translocation of high-mobility group box 1 (HMGB1) and nuclear factor kappa B (NF-κB) [30]. However, the effect of curcumin on NASH-HCC to precisely understand the anticancer mechanism in an inflammatory setting is poorly investigated.

The overall goal of the present study was to investigate the preventive effect of curcumin on NASH-associated liver tumorigenesis and explore its underlying molecular mechanisms. To achieve this, we employed the experimental NASH-HCC model developed by Friedman's group, which is a fully characterized murine model that recapitulates the disease progression from steatohepatitis to fibrosis and HCC and closely resembles the metabolic, histological, and transcriptomic signature of human NASH-HCC. Using this model, we demonstrated that curcumin treatment attenuates the progression of NASH to HCC by ameliorating inflammation and fibrosis. In terms of the underlying mechanisms, our data suggest that curcumin exerts preventive effects on HCC development by suppressing AATF expression via kruppel-like factor 4 (KLF4) and the specificity protein 1 (Sp1) signaling pathway. Taken together, these provide novel data demonstrating the hepatoprotective action of curcumin and its therapeutic role in the treatment of NASH-associated HCC.

2. Materials and Methods

2.1 *Materials*

Curcumin, carboxy methyl cellulose (CMC), TRIzol, RIPA buffer, Sirius Red stain, corn oil, and AATF antibody were procured from Sigma-Aldrich (St. Louis, USA). Dulbecco's modified eagle's medium (DMEM), hematoxylin, DMSO, glucose, and fructose were procured from HiMedia Laboratories (India). Lipofectamine 3000, penicillin/streptomycin, glutamine, and FBS were from Invitrogen (USA); antibodies to Sp1, pJNK, pErk1/2, JNK, Erk1/2, and control and AATF shRNA from Santa Cruz Biotechnology, Inc. (CA, USA); antibodies to KLF4, Ki67, pSTAT3, STAT3, and β-actin from Cell Signaling Technologies (USA); verso cDNA synthesis kit, and DyNamo Colorflash SYBR green kit from Thermo Fisher Scientific (USA); western bright ECL HRP substrate from Advansta (USA); western blotting materials were from Bio-Rad; primers from Integrated DNA Technologies (IDT) (Iowa, USA), water-soluble tetrazolium salt (WST-1) (Takara, India). The western diet was customized and purchased from Research Diets Inc. (NJ, USA). The ALT, AST, and Total cholesterol kits were from Monlab tests (Spain) and all other reagents were obtained from Thermo Fisher Scientific or Sigma.

2.2 *Animals*

Male C57Bl/6NCrl mice (6-7 weeks old) were purchased from Hylasco Biotechnology Pvt. Ltd. (Charles River Laboratories) and maintained as described previously [31]. All the mice were housed in a 12-hour light and 12-hour dark cycle in the animal facility of the Center for Experimental Pharmacology and Toxicology, JSS AHER. All the procedures were performed according to the protocol approved by the Committee for the Purpose of Control and Supervision of Experiments on Animals (CPCSEA), Govt. of India (JSSAHER/CPT/IAEC/060/2021).

2.3 *Study design and interventions*

Following the one-week acclimatization, mice were fed either a chow diet (CD, lab diet, USA) with normal water (NW) or a high fat, high sucrose, and high cholesterol (WD, 21% fat, 41% sucrose, and 1.25% cholesterol by weight, Research Diet, Inc., USA) diet with sugar water (SW, 18.9 g/L d-glucose and 23.1 g/L d-fructose) ad libitum for the first 12 weeks. Simultaneously with dietary intervention, all the mice were treated with CCl4 at a dose of 0.2 µl/g of body weight dissolved in corn oil and administered intraperitoneally once a week throughout the study as described previously [32]. After 12 weeks, mice were randomly divided into four groups: CDNW with vehicle (0.5% CMC), CDNW with curcumin (100 mg/kg/day), WDSW with vehicle (0.5% CMC), and WDSW with curcumin (100 mg/kg/day) **(Figure 1A)**. Curcumin and vehicle were administered every day for 12 weeks via oral gavage. Mice were continuously monitored for food intake, water intake, and body weight. After 24 weeks, mice were euthanized, and blood and tissues were collected for further analysis.

2.4 *Biochemical analysis*

The blood collected via the retro-orbital puncture route from the overnight fasted mice was processed by centrifuging at 1500 g for 15 minutes at 4^0C. The serum collected was stored at -80^0C. Serum ALT, AST, and Total cholesterol were measured according to the manufacturer's instructions [33].

2.5 *Liver Histology*

Formalin-fixed, paraffin-embedded liver tissues were stained with hematoxylin and eosin (H&E) staining to evaluate liver histology for steatosis, lobular inflammation, and hepatocyte ballooning. NAFLD activity scoring (NAS) was evaluated by an expert pathologist (double blindfolded) at JSS Hospital according to the FLIP algorithm and NASH-Clinical Research Network (CRN) criteria [34,35].

2.6 *Sirius Red Staining*

The formalin-fixed, paraffin-embedded liver tissue sections were deparaffinized and rehydrated using xylene and a series of ethanol concentrations. Slides were stained with hematoxylin for 10 minutes. Following a water wash, the slides were stained by Sirius red solution for 1 hour at room temperature. The excess stain was removed by washing it in 0.5% acidified water for 5 minutes. Slides were mounted with coverslips, and the images were taken with an Olympus BX53 microscope and quantified using the ImageJ software.

2.7 *Immunostaining*

The formalin-fixed, paraffin-embedded liver tissue sections were deparaffinized and rehydrated using xylene and a series of ethanol concentrations. Slides were incubated with citrate buffer (pH 6) for 15 minutes at 94^0C for antigen retrieval, followed by a water wash and incubation with 3% hydrogen peroxide for 10 min. After the incubation with blocking buffer for 1 h at room temperature, sections were added with the target of interest and incubated overnight at 4°C in a humidified chamber. Polyexcel HRP/DAB detection system-one step (PathnSitu, Biotechnologies) was

used for developing the signals and hematoxylin for counterstaining the nucleus. Antibody dilution for AATF (1:100) and Ki67 (1:200). All the images were taken using an Olympus BX53 microscope and quantified using the ImageJ software.

2.8 *RNA isolation and quantitative real-time PCR*

Total RNA was isolated from the cells and liver tissues using the TRIzol reagent according to the manufacturer's protocol. The RNA was quantified using a nanodrop spectrophotometer and reverse transcribed using a Verso cDNA synthesis kit. Gene expression analysis was carried out in the Rotor-Gene Q 5plex HRM System (QIAGEN) using the DyNamo Colorflash SYBR Green kit, 0.5 mM primers, and 50 ng of cDNA in a 20 µl reaction volume. The relative fold change in gene expression was calculated as $2^{-\Delta\Delta Ct}$ and relative fold changes were calculated by normalizing the values to internal control, β actin.
The validated primer sequences used are as follows: mouse IL-1β (Forward primer 5`-TGCCACCTTTTGACAGTGATGA-3` and Reverse primer 5`TGATGTGCTGCTGCGAGATTTG-3`); mouse IL-6 (Forward primer 5`-GGAGCCCACCAAGAACGATA-3` and Reverse primer 5`-AACTGGATGGAAGTCTCTTGC-3`); mouse TNF-α (Forward primer 5`-TAGCCCACGTCGTAGCAAACC-3` and Reverse primer 5`-CTTTGAGATCCATGCCGTTGGC-3`); mouse α-SMA (Forward primer 5`-CTACTGCCGAGCGTGAGATTGT-3` and Reverse primer 5`-CCCGCTGACTCCATCCCAATGA-3`); mouse TGF-β (Forward primer 5`-GCTGCATATCGTCCTGTGG-3` and Reverse primer 5`-CTTCCATTTCCACATCCGACT-3`); mouse CD31 (Forward primer 5`-GTGGAAGTGTCCTCCCTTGA-3` and Reverse primer 5`-GGGAGCCTTCCGTTCTAGAGTAT-3`); mouse AFP (Forward primer 5`-AACCTCCAGGCAACAACCATT-3` and Reverse primer 5`-CACTCCTCGTGGATGTGAGC-3`); human AATF (Forward primer 5`-TAGAACGGAAGACCAGCTCC-3` and Reverse primer 5`-TGCTAAGGACATGAAACCGA-3`, mouse AATF (Forward primer 5`-GAGTGATGATGCCAGGACGGA-3` and Reverse primer 5`-ACTGTCACTTCCCACGGTCTG-3`); human KLF4 (Forward primer 5`-GATGCTCACCCCACCTTCTTC-3` and Reverse primer 5`-GTAAGGTTTCTCACCTGTGTGG-3`, mouse KLF4 (Forward primer 5`-CACCTGGCGAGTCTGACAT-3` and Reverse primer 5`-TTCCTCACGCCAACGGTTA-3`); human Sp1 (Forward primer 5`-CCACCATGAGCGACCAAGAT-3` and Reverse primer 5`-AAGGCACCACCACCATTACC-3`; mouse Sp1 (Forward primer 5`-GCCACCATGAGCGACCAAGAT-3` and Reverse primer 5`-GCCAGCAGAGCCAAAGGAGAT-3`); human β-actin (Forward primer 5`-AGAGATGGCCACGGCTGCTT -3` and Reverse primer 5`-CAGGACTCCATGCCCAGGAA-3`; mouse β-actin (Forward primer 5`-CAGCCTTCCTTCTTGGGTATGG-3` and Reverse primer 5`-CCTGCTTGCTGATCCACATCT-3`)

2.9 *Immunoblotting*

Fresh lysates were prepared from the cells and liver tissues using RIPA buffer containing protease/phosphatase inhibitors. The supernatants were collected after centrifuging the homogenate at 13000 rpm for 10 minutes at 4^0C. The protein

concentration of the lysates was determined by Bradford's protein estimation method. An equal amount of lysates (30 µg) were loaded into SDS-PAGE to separate the protein and transferred onto a nitrocellulose membrane. Further, the membranes were blocked with 5% non-fat skim milk for 1 hour and incubated with the target primary antibodies (AATF, pJNK, JNK, pErk1/2, Erk1/2, KLF4, Sp1, pSTAT3, STAT3 and β-actin) overnight at 4^0C. Following this, the membrane was incubated with a secondary antibody for 2 h at room temperature. Western Bright ECL HRP substrate was used to visualize the blots in the UVitec Alliance Q9 chemiluminescence imaging system. Images were analyzed using ImageJ software and bands were normalized with corresponding internal controls.

2.10 *Cell culture and generation of stable cell lines*

Human HCC cell line - QGY-7703 (a kind donation from Dr. Devanand Sarkar, Virginia Commonwealth University, Richmond, USA) was cultured in Dulbecco's modified eagle's medium containing 4.5 g/L glucose and supplemented with 10% fetal bovine serum, L-glutamine, and 100 U/ml penicillin-streptomycin incubated at 37^0C in 5% CO_2.
In QGY-7703 cells, AATF shRNA expressing stable clones were generated as previously described [21]. Different concentrations of puromycin (1-10 µg/ml) were used to determine the optimal antibiotic concentration for selecting stable cell colonies. According to the manufacturer's instructions, the control and AATF shRNA plasmids containing the puromycin resistance gene were transfected into QGY-7703 cells. Single colonies were then chosen and grown in 1 µg/ml puromycin. AATF knockdown was confirmed by both qRT-PCR and immunoblotting analysis.

2.11 *Cell viability assay*

The effect of curcumin on cell viability was determined by the WST-1 assay. Briefly, $1x10^4$ cells were seeded into a 96-well plate and allowed to attain 70% confluency. Different concentrations of curcumin (0, 10, 20, 40, 60, 80, and 100 µM) dissolved in DMSO were treated in cells for 24 h, 48 h, and 72 h. The final concentration of DMSO in the treatment medium was < 0.05%. To assess the cell viability, control and AATF knockdown QGY 7703 cells were treated with curcumin (20 µM/ml) for 24 hours. At the end of the treatment, a 1:10 diluted WST-1 mix solution was added to each well and incubated for 60 minutes at 37^0C in 5% CO_2. The absorbance was measured at 450 nm on a multi-mode plate reader (EnSpire™ Multimode Plate Reader, Perkin Elmer). The data is represented as percent cell viability after normalizing with a negative control (no treatment).

2.12 *Migration assay*

QGY 7703 control and AATF knockdown cells were seeded at a density of $5x10^5$ in a 6-well plate and cultured up to 70% confluency. A gentle scratch was done using a 1000 µl pipette tip across the center of each well. The detached cells were removed with PBS. Cells were incubated with either vehicle or curcumin (20 µM/ml) containing fresh media. After 24 h, cells were observed under the microscope for migration ability. The images were taken using a Zeiss Primovert inverted microscope, and the gap distance was measured using ImageJ software.

2.13 *Statistical analysis*

Results were calculated as mean +/- SEM. Statistical significance was analyzed using Student's t-test for two groups or analysis of variance (ANOVA) with post hoc Bonferroni correction for multiple comparisons. All statistical analyses were performed using the GraphPad Prism software (version 6), and p values < 0.05 (*/#) or < 0.001 (**/##) were considered significant.

3. Results

3.1 Curcumin attenuates the progression of NASH to HCC

To assess the effect of curcumin treatment on NASH-associated HCC, a 24-week study was performed on C57Bl/6 mice. Mice were divided into two groups and fed with either chow diet normal water (CDNW) or western diet sugar water (WDSW). Both groups received a low dose of CCl4 (0.2 µl/g body weight) intraperitoneally once a week until the end of the study. In the 12th week, upon confirmation of NASH in the WDSW/CCl_4 group, the mice were further divided into 4 groups: CDNW/CCl_4 + vehicle control (VC), CDNW/CCl_4 + curcumin (100 mg/kg body weight), WDSW/CCl_4 + vehicle, and WDWW/CCl_4 + curcumin (100 mg/kg body weight) (**Figure 1A**). The mice treated with vehicle in WDSW/CCl_4 gained significant body weight and liver weight compared to CDNW/CCl_4 mice (**Figure 1B and 1C**). This was consistent with hypercholesteremia and elevated liver enzymes in mice treated with vehicle in WDSW/CCl_4, thereby confirming severe liver injury **(Figure 1D, 1E, and 1F)**. Curcumin treatment in the WDSW/CCl_4 mouse groups for 12 weeks showed a notable reduction in both body weight and liver weight compared to the vehicle treated WDWW/CCl_4 mice (**Figure 1B and 1C**). Similarly, ALT, AST, and total cholesterol levels were also lowered by curcumin treatment in WDSW/CCl_4 mice **(Figure 1D, 1E, and 1F)** when compared to CDNW/CCl_4 mice. No effects were seen in CDNW/CCl_4 mouse groups treated with curcumin. Additionally, the administration of curcumin also had considerable effects on fasting glucose and fasting insulin levels **(Figure 1G and 1H)**, along with HOMA-IR in WDSW/CCl_4 mice **(Figure 1I)**. Thus, these data demonstrate that curcumin treatment ameliorated obesity, insulin resistance, and liver injury in the WDWW/CCl_4 mouse groups.

Histological examinations were carried out for all four groups of mice. Consistent with previous data, CDNW/CCl_4 mice did not develop steatosis, inflammation, and hepatocyte ballooning in 24 weeks time. Severe steatosis and steatohepatitis were observed in vehicle treated WDSW/CCl_4 mice. Curcumin treatment drastically improved the NASH features in WDSW/CCl_4 mouse groups and showed no and/or adverse effects on CDNW/CCl_4 mice **(Figure 2A and 2B)**. WDSW/CCl_4 mice with vehicle control showed evident NASH development with marked steatosis (2.8±0.2), hepatocellular ballooning (1.9±0.12), and lobular inflammation (2.4±0.24) with a NAFLD activity score of 7.8±0.3. As hypothesized, curcumin treatment showed a significant improvement in NASH hallmarks with a notable reduction in steatosis (1.4+/-0.2), hepatocellular ballooning (1.2±0.2), and lobular inflammation (1.4±0.24) with NAFLD activity score of 3.7±0.4 in WDSW/CCl_4 mice **(Figure 2C to 2F)**. Numerous tumors (8-10 per mouse) were observed on the liver surface in 7 out of 8 mice treated with vehicle in WDSW/CCl_4, while very few (1-2 per mouse) to no

tumors in curcumin treated WDSW/CCl_4 mouse groups **(Figure 2A, 2G and 2H)**. Taken together, these data suggest that curcumin treatment improves NASH liver histology and attenuates the progression of NASH to HCC.

3.2 Curcumin ameliorates inflammation, fibrosis and tumorigenesis in experimental NASH-HCC

Next, we examined the effect of curcumin on liver inflammation, a key player in NASH settings. Proinflammatory cytokines such as interleukin-1β (IL-1β), interleukin -6 (IL-6), and tumor necrosis factor α (TNFα) that were overexpressed in vehicle treated WDSW/CCl_4 mice were reduced upon the administration of curcumin, marking its anti-inflammatory effects **(Figure 3A, 3B, and 3C)**. Further, the stress-responsive mitogen-activated protein kinases (MAPKs) activated due to these proinflammatory cytokines were examined. Curcumin administration downregulated the phosphorylation of extracellular signal-regulated protein kinase (ERK1/2) and c-Jun N-terminal kinase (JNK) compared to WDSW/CCl_4 mouse groups with vehicle control **(Figure 3D and 3E)**.

Sirius red staining of liver sections was performed for all the groups to examine the effect of curcumin on liver fibrosis. WDSW/CCl_4 mice with vehicle control showed significant fibrosis, which was reduced, in curcumin-treated mice **(Figure 4A and 4B)**. Further, curcumin reduced the activation of hepatic stellate cells as determined by the mRNA expression of alpha-smooth muscle actin (αSMA) **(Figure 4C)**. The major fibrogenic gene, transforming growth factor β (TGF β) was also reduced in curcumin-treated WDSW/CCl_4 mice compared to vehicle control **(Figure 4D)**.

Additionally, we also verified the preventive effect of curcumin on liver tumorigenesis initiated by NASH by immunostaining of the proliferative marker Ki67 and observed that curcumin-treated mice livers showed negative Ki67 immunostaining against positive staining in WDSW/CCl_4 mice with vehicle control **(Figure 4E and 4F)**. We then investigated the mRNA levels of cluster of differentiation 31 (CD31), a specific marker for vascular differentiation, and alpha-fetoprotein (AFP), a key biomarker of HCC. Curcumin treatment downregulated both CD31 and AFP expression levels compared to WDSW/CCl_4 mice with vehicle alone **(Figure 4G and 4H)**. Collectively, these data provide evidence that curcumin treatment improves WDSW/CCl_4-induced inflammation and fibrosis and prevents NASH-associated liver tumorigenesis.

3.3 Curcumin treatment suppresses AATF-mediated NASH-HCC

Next, we wanted to understand the possible molecular targets of curcumin in preventing NASH-HCC. Owing to this objective, our previous findings have shown elevated levels of AATF in NASH-associated HCC in a diet-induced animal model of NAFLD (DIAMOND) [21]. AATF, an oncogenic gene overexpressed in many cancers, including HCC [22], is responsible for the activation of key signaling molecules involved in tumorigenesis. Thus, in this study, we investigated the effect of curcumin on AATF levels in NASH-HCC. The immunostaining and mRNA expressions of AATF were significantly reduced upon curcumin treatment when compared to vehicle control in WDSW/CCl_4 mouse groups **(Figure 5A and 5B)**. To

determine the non-toxic but effective concentrations of curcumin against human HCC cells, cell viability assay was performed. Curcumin treatment affected the cell viability of QGY-7703 cells in a dose- and time-dependent manner within 24 hours of exposure in contrast to the control group (**Figure 5C and 5D**). Furthermore, to understand the specific effect of curcumin on AATF, we used stable clones of control and AATF knockdown QGY-7703 cells. We observed that AATF expression upon curcumin treatment was reduced in control QGY-7703 cells, but no changes were seen in AATF knockdown QGY-7703 cells **(Figures 5E and 5F)**. Furthermore, we evaluated the proliferative activity and migration ability of the control and AATF knockdown QGY-7703 cells upon treatment with curcumin **(Figure 5G and 5H)**. Interestingly, curcumin showed a similar inhibitory effect as that of AATF knockdown cells on the proliferation and migration of human HCC cells. These results demonstrated that curcumin treatment could suppress AATF expression in NASH-HCC and thereby prevent tumorigenesis.

3.4 Molecular mechanism of AATF inhibition by Curcumin

Further, we sought to explore the possible mechanisms of curcumin-mediated downregulation of AATF. Previous studies have demonstrated that curcumin treatment demethylates the CpG islands of the promoter of KLF4, increasing its expression [36]. Thus, we evaluated the expression of KLF4 in the mouse liver tissue of all four groups. Interestingly, KLF4 was upregulated in curcumin-treated WDSW/CCl_4 mice in contrast to vehicle alone **(Figure 6A and 6C)**. KLF4, being a tumor suppressor gene, is implicated in the downregulation of several oncogenes in HCC. Studies have shown that KLF4 negatively regulates the expression of Sp1, a pro-oncogenic molecule that binds directly to the AATF promoter and induces its expression [37,16]. Following this hypothesis, in our study, curcumin treatment showed a marked reduction in Sp1 levels in the WDSW/CCl_4 mouse groups compared to vehicle control **(Figure 6B and 6C)**. Similarly, the human HCC cells, QGY-7703 cells upon treatment with curcumin also showed upregulated levels of KLF4 **(Figure 6D and 6E)**. This was supported by the downregulation of Sp1 in the QGY-7703 cells treated with curcumin **(Figures 6F and 6G)**. Overall, these data indicate that curcumin via KLF4 inhibits the expression of Sp1, which in turn is responsible for the downregulation of AATF. Next, we evaluated the levels of activated STAT3, a prominent transcription factor that plays a key role in the progression and metastasis of HCC [38]. As anticipated, the pSTAT3 levels were downregulated in curcumin treated WDSW/CCl_4 mice compared to the vehicle control **(Figure 6H).** Similarly, pSTAT3 levels were reduced in curcumin-treated control QGY-7703 cells in contrast to AATF knockdown cells **(Figure 6I)**. Overall, the data indicate that curcumin-mediated AATF inhibition prevents the disease progression of NASH to HCC.

4. Discussion

HCC, a type of liver malignancy, has a high mortality rate, and current treatment options are limited and often ineffective [39]. NAFLD is the fastest-growing cause of the rising prevalence of HCC. Apart from the linear progression of NASH to fibrosis, cirrhosis, and HCC, recent studies have shown the occurrence of HCC in patients without cirrhosis as well [3]. The complex process of NASH progressing in HCC is linked to the metabolic, immunological, and inflammatory milieu induced by insulin

resistance and lipotoxicity [8]. Due to poor prognosis and limited studies on molecular pathogenesis, NASH-associated HCC management is a challenge. There are no approved drugs to treat NASH-HCC despite it being a leading etiology for oncogenesis. Added to this, NASH-HCC is a difficult disease to treat, and patients often have poor outcomes due to late diagnosis and limited treatment options [11]. Therefore, there is a critical need for the development of effective therapeutic agents to target NASH-HCC. These agents should be able to specifically target cancer cells and minimize damage to healthy cells, thereby potentially improving outcomes, increasing survival rates, and reducing the burden of this devastating disease.

There are a number of natural therapeutic agents that have been explored for the treatment of HCC [40]. Natural therapeutic agents, such as herbs, extracts, or dietary supplements, have gained significant attention in the treatment of HCC due to their potential anti-cancer properties [41,42]. Using natural therapeutic agents for treatment can be beneficial for several reasons. Firstly, natural agents are typically less toxic than conventional chemotherapeutic drugs, which can cause significant side effects. Secondly, natural agents can be used in combination with traditional treatments such as surgery, radiation, and chemotherapy to enhance their efficacy and reduce side effects. Finally, natural agents are often more affordable and accessible than conventional drugs, making them an attractive option for patients who cannot afford expensive treatments. Overall, the use of natural therapeutic agents in the treatment of HCC can be a safe and effective option for patients looking to manage their cancer symptoms and improve their overall quality of life. Along the same lines, curcumin is one such naturally occurring compound that is well known for its efficacy and safety [26]. It has been studied for its potential health benefits, and research suggests that it may have a variety of targets in the human body. Some of the targets of curcumin include inflammation, oxidative stress, cancer, brain function, and heart health [27,43,44]. There is growing evidence from both preclinical and clinical studies that suggests curcumin may have anti-cancer effects against HCC by exerting anti-inflammatory effects, apoptosis, and anti-angiogenic effects [30,45,46]. However, less is explored in the area of NASH-HCC. Studies have suggested that curcumin may help reduce liver inflammation and oxidative stress, which are key factors in the development and progression of NASH [10]. Additionally, curcumin has been found to have beneficial effects on lipid metabolism, insulin resistance, gut microbiota, and fibrosis, all of which are associated with NASH and potentially the progression of NASH to HCC [5]. However, the potential therapeutic role of curcumin in NASH-HCC needs further validation.

There are several murine models of NASH and NASH-HCC, but most do not recapitulate the human disease, which is a major drawback [47]. In this study, we have used a murine model of NASH that could be induced with a simple diet and chemical, which progresses through the stages of steatosis, steatohepatitis, fibrosis, and liver cancer [32]. Of note, this experimental model employs intraperitoneal injection of a very low dose of CCl_4 (0.2 µl/g) once per week, starting simultaneously with diet administration. The WDSW consists of a high fat, high sucrose, and high cholesterol diet (WD, 21% fat, 41% sucrose, and 1.25% cholesterol by weight) with sugar water (SW, 18.9 g/L d-glucose and 23.1 g/L d-fructose). The disease development in the WDSW/CCl_4 FAT-NASH (**F**ibrosis **A**nd **T**umors) murine model closely resembles the metabolic, histological, and transcriptomic signature of human

NASH-HCC, making the study more significant and translational. Herein, we evaluated the hepatoprotective effect of curcumin using this experimental NASH-HCC model. Interestingly, we found that mice treated with vehicle in WDSW/CCl_4 for 24 weeks readily developed HCC with numerous visible tumors on the liver. Previously, studies by Afrin R et al., demonstrated that curcumin would reduce the progression of NASH to HCC by inhibiting the cytosolic translocation of high mobility group box 1 (HMGB1) and the nuclear translocation of NF-κB using a streptozotocin-HFD-induced NASH-HCC mouse model [30]. Similarly, curcumin treatment in our study attenuated tumor formation by improving WDSW-induced obesity and liver damage. The treatment of curcumin to the WDSW/CCl_4 mice resulted in an improvement in obesity, as marked by a reduction in body weight and liver weight. Furthermore, the study demonstrated amelioration in insulin resistance and marked improvement in the biochemical and histological outcomes after treatment with curcumin in the WDSW/CCl_4 mouse groups. Studies have reported that inflammatory cytokines TNF-α, and IL-6 targeting JNK, ERK, and NF-κB pathways drive HCC arising in inflammatory settings [10,48]. Curcumin treatment successfully lessened the inflammatory cytokines as well as stress kinases. It is well established that inflammatory setting gives rise to or predisposes to fibrosis and HCC. The cytokine-driven interactions between the stellate cells and the creation of the microenvironment lead to the emergence of HCC development [49]. In this regard, in our experiments, we found that the elevated expression of fibrogenic genes and oncogenic markers in WDSW/CCl_4 mice was reduced upon treatment with curcumin. Collectively, our study reports the effect of curcumin on attenuating the progression of NASH to HCC while also improving the existing NASH condition.

The current study provides insight into the mechanisms by which curcumin prevents NASH-associated hepatocarcinogenesis. Curcumin has been found to inhibit the activation of oncogenes and also induce apoptosis in HCC cells. It has also been shown to have anti-inflammatory effects, which can help prevent the development of HCC [24,43]. Furthermore, we examined the effect of curcumin on AATF, an oncogene overexpressed in NASH-HCC. Interestingly, our data showed that curcumin treatment downregulated AATF expression in mouse liver tissues. In order to elucidate the molecular mechanisms of how curcumin acts on AATF, stable clones of AATF control and AATF knockdown were prepared in human HCC cells, QGY-7703. The oncogenic properties of the QGY-7703 cells, such as increased cell proliferation, and cell migration were inhibited upon curcumin treatment in control cells and had no effect on the AATF knockdown cells. Studies by Chatterjee B. et al., have demonstrated that KLF4, a key player in regulating cell growth, differentiation, and development, is activated by curcumin. Demethylation of CpG islands on the KLF4 promoter by curcumin is known to increase its expression and also its promoter occupancy to p21, leading to curcumin-mediated cell cycle arrest and inhibition of cell proliferation [36]. Similarly, our studies showed a significant increase in the expression of KLF4 in WDSW/CCl_4 mice treated with curcumin compared to vehicle controls. Consistently, upon curcumin treatment, there was upregulation of KLF4 in AATF control QGY-7703 cells. In another study by Kanai M. et al., loss of KLF4 leads to sp1 overexpression and promotes the development and progression of human gastric cancer [37]. Thus, KLF4 negatively regulates the expression of Sp1, a pro-oncogenic molecule that binds directly to the AATF promoter and induces its expression. Consistent with these studies, we found that in WDSW/CCl_4 mice and AATF control cells, curcumin treatment reduced AATF expression by

downregulating Sp1 via KLF4 and thereby exerting anti-tumor activity. It is reported that STAT3 plays a key oncogenic role in cell proliferation, migration, immune suppression, and the angiogenesis of HCC [38]. Studies by Kumar et al., have shown that AATF drives HCC via monocyte chemoattractant protein 1 (MCP1) and STAT3 [21]. Interestingly, p-STAT3 levels were upregulated in the liver of curcumin-treated mice and curcumin-treated AATF control cells compared to vehicle and AATF knockdown cells, respectively.

In conclusion, the current study adds to the growing body of evidence supporting the promising role of curcumin and its potential applications in the prevention and treatment of NASH-HCC. We demonstrated that curcumin ameliorates AATF-mediated liver damage and inflammation to cancer in NASH-HCC via KLF4 and Sp1 signaling pathway. Furthermore, the study offers valuable insight into the potential benefits of curcumin for NASH-HCC, for which the development of effective therapeutic agents is an absolute necessity, and additionally provides a basis for more rigorous clinical trials to fully evaluate the effectiveness of curcumin for NASH-HCC.

CRediT authorship contribution statement

Akshatha N. Srinivas and Diwakar S.: Writing- original draft, Investigation, Methodology, Formal Analysis, Visualization. Saravana Babu Chidambaram: Writing- review & editing. Prasanna K. Santhekadur: Formal analysis, Writing- review & editing. Divya P. Kumar- Funding acquisition, Supervision, Conceptualization, Project administration, Formal analysis, Writing- original draft.

Declaration of Competing Interest

The authors declare that they have no known competing financial interests or personal relationships that could have appeared to influence the work reported in this paper.

Funding

This study was supported in whole or in part, by the Ramalingaswami Re-entry Fellowship from the Department of Biotechnology (Grant No.: BT/RLF/Re entry/58/2017), Extramural Ad-hoc Grant from the Indian Council of Medical Research (ICMR) (Grant No.: 5/3/8/55/2020-ITR) to DPK, and Senior Research Fellowship (SRF) from ICMR to ANS. The authors also acknowledge funding support from the Department of Science and Technology's Promotion of University Research and Scientific Excellence (DST-PURSE: SR/PURSE/2018/81c).

References

1. Llovet JM, Kelley RK, Villanueva A, et al. Hepatocellular carcinoma. *Nat Rev Dis Primers.* 2021;7(1):6. doi:10.1038/s41572-020-00240
2. Rumgay H, Arnold M, Ferlay J, et al. Global burden of primary liver cancer in 2020 and predictions to 2040. *J Hepatol.* 2022;77(6):1598-1606. doi:10.1016/j.jhep.2022.08.021
3. Ioannou GN. Epidemiology and risk-stratification of NAFLD-associated HCC. *J Hepatol.* 2021;75(6):1476-1484. doi:10.1016/j.jhep.2021.08.012
4. Suresh D, Srinivas AN, Kumar DP. Etiology of Hepatocellular Carcinoma: Special Focus on Fatty Liver Disease. Front Oncol. 2020;10:601710. doi:10.3389/fonc.2020.601710
5. Kutlu O, Kaleli HN, Ozer E. Molecular Pathogenesis of Nonalcoholic Steatohepatitis- (NASH-) Related Hepatocellular Carcinoma. *Can J Gastroenterol Hepatol.* 2018;2018:8543763. Published 2018 Aug 29. doi:10.1155/2018/8543763
6. Stine JG, Wentworth BJ, Zimmet A, et al. Systematic review with meta-analysis: risk of hepatocellular carcinoma in non-alcoholic steatohepatitis without cirrhosis compared to other liver diseases. *Aliment Pharmacol Ther.* 2018;48(7):696-703. doi:10.1111/apt.14937
7. Pinyol R, Torrecilla S, Wang H, et al. Molecular characterisation of hepatocellular carcinoma in patients with non-alcoholic steatohepatitis. *J Hepatol.* 2021;75(4):865-878. doi:10.1016/j.jhep.2021.04.049
8. Llovet JM, Willoughby CE, Singal AG, et al. Nonalcoholic steatohepatitis-related hepatocellular carcinoma: pathogenesis and treatment [published online ahead of print, 2023 Mar 17]. Nat Rev Gastroenterol Hepatol. 2023 doi:10.1038/s41575-023-00754-7
9. Banini BA, Kumar DP, Cazanave S, et al. Identification of a Metabolic, Transcriptomic, and Molecular Signature of Patatin-Like Phospholipase Domain Containing 3-Mediated Acceleration of Steatohepatitis. Hepatology. 2021;73(4):1290-1306. doi:10.1002/hep.31609
10. Yang YM, Kim SY, Seki E. Inflammation and Liver Cancer: Molecular Mechanisms and Therapeutic Targets. *Semin Liver Dis.* 2019;39(1):26-42. doi:10.1055/s-0038-1676806
11. Anstee QM, Reeves HL, Kotsiliti E, Govaere O, Heikenwalder M. From NASH to HCC: current concepts and future challenges. *Nat Rev Gastroenterol Hepatol*. 2019;16(7):411-428. doi:10.1038/s41575-019-0145-7

12. Srinivas AN, Suresh D, Mirshahi F, Santhekadur PK, Sanyal AJ, Kumar DP. Emerging roles of AATF: Checkpoint signaling and beyond. *J Cell Physiol*. 2021;236(5):3383-3395. doi:10.1002/jcp.30141

13. Bruno T, De Angelis R, De Nicola F, et al. Che-1 affects cell growth by interfering with the recruitment of HDAC1 by Rb. *Cancer Cell.* 2002;2(5):387-399. doi:10.1016/s1535-6108(02)00182-4

14. Bruno T, De Nicola F, Iezzi S, et al. Che-1 phosphorylation by ATM/ATR and Chk2 kinases activates p53 transcription and the G2/M checkpoint. *Cancer Cell*. 2006;10(6):473-486. doi:10.1016/j.ccr.2006.10.012

15. Page G, Lödige I, Kögel D, Scheidtmann KH. AATF, a novel transcription factor that interacts with Dlk/ZIP kinase and interferes with apoptosis. *FEBS Lett.* 1999;462(1-2):187-191. doi:10.1016/s0014-5793(99)01529-x

16. Kaul D, Mehrotra A. Functional characterization of AATF transcriptome in human leukemic cells. *Mol Cell Biochem.* 2007;297(1-2):215-220. doi:10.1007/s11010-006-9317-1

17. Haanpää M, Reiman M, Nikkilä J, Erkko H, Pylkäs K, Winqvist R. Mutation analysis of the AATF gene in breast cancer families. *BMC Cancer.* 2009;9:457. Published 2009 Dec 21. doi:10.1186/1471-2407-9-457

18. Guo Q, Xie J. AATF inhibits aberrant production of amyloid beta peptide 1-42 by interacting directly with Par-4. *J Biol Chem.* 2004;279(6):4596-4603. doi:10.1074/jbc.M309811200

19. Welcker D, Jain M, Khurshid S, et al. AATF suppresses apoptosis, promotes proliferation and is critical for Kras-driven lung cancer. *Oncogene.* 2018;37(11):1503-1518. doi:10.1038/s41388-017-0054-6

20. Di Padova M, Bruno T, De Nicola F, et al. Che-1 arrests human colon carcinoma cell proliferation by displacing HDAC1 from the p21WAF1/CIP1 promoter. *J Biol Chem.* 2003;278(38):36496-36504. doi:10.1074/jbc.M306694200

21. Kumar DP, Santhekadur PK, Seneshaw M, Mirshahi F, Uram-Tuculescu C, Sanyal AJ. A Regulatory Role of Apoptosis Antagonizing Transcription Factor in the Pathogenesis of Nonalcoholic Fatty Liver Disease and Hepatocellular Carcinoma. *Hepatology.* 2019;69(4):1520-1534. doi:10.1002/hep.30346

22. Preprint: Suresh D, Srinivas AN, Prashant A, Satish S, Vishwanath P, Santhekadur PK, Kumar DP. AATF Inhibition Exerts Antiangiogenic Effects Against Human Hepatocellular Carcinoma. bioRxiv 2022.11.28.518287; doi: https://doi.org/10.1101/2022.11.28.518287

23. Shao G, Liu Y, Lu L, et al. The Pathogenesis of HCC Driven by NASH and the Preventive and Therapeutic Effects of Natural Products. *Front Pharmacol*. 2022;13:944088. Published 2022 Jul 7. doi:10.3389/fphar.2022.944088

24. Aggarwal BB, Harikumar KB. Potential therapeutic effects of curcumin, the anti-inflammatory agent, against neurodegenerative, cardiovascular, pulmonary, metabolic, autoimmune and neoplastic diseases. *Int J Biochem Cell Biol.* 2009;41(1):40-59. doi:10.1016/j.biocel.2008.06.010

25. de Waure C, Bertola C, Baccarini G, Chiavarini M, Mancuso C. Exploring the Contribution of Curcumin to Cancer Therapy: A Systematic Review of Randomized Controlled Trials. *Pharmaceutics.* 2023;15(4):1275. doi:10.3390/pharmaceutics15041275

26. Hewlings SJ, Kalman DS. Curcumin: A Review of Its Effects on Human Health. *Foods.* 2017;6(10):92. doi:10.3390/foods6100092

27. Kunnumakkara AB, Bordoloi D, Harsha C, Banik K, Gupta SC, Aggarwal BB. Curcumin mediates anticancer effects by modulating multiple cell signaling pathways. *Clin Sci (Lond).* 2017;131(15):1781-1799. doi:10.1042/CS20160935

28. Kim BH, Lee ES, Choi R, et al. Protective Effects of Curcumin on Renal Oxidative Stress and Lipid Metabolism in a Rat Model of Type 2 Diabetic Nephropathy. Yonsei Med J. 2016;57(3):664-673. doi:10.3349/ymj.2016.57.3.664

29. Ramirez-Tortosa MC, Ramirez-Tortosa CL, Mesa MD, Granados S, Gil A, Quiles JL. Curcumin ameliorates rabbits's steatohepatitis via respiratory chain, oxidative stress, and TNF-alpha. *Free Radic Biol Med.* 2009;47(7):924-931. doi:10.1016/j.freeradbiomed.2009.06.015

30. Afrin R, Arumugam S, Rahman A, et al. Curcumin ameliorates liver damage and progression of NASH in NASH-HCC mouse model possibly by modulating HMGB1-NF-κB translocation. *Int Immunopharmacol.* 2017;44:174-182. doi:10.1016/j.intimp.2017.01.016

31. Srinivas AN, Suresh D, Suvarna D, et al. Unraveling the Potential Role of Tecomella undulata in Experimental NASH. Int J Mol Sci. 2023;24(4):3244. Published 2023 Feb 7. doi:10.3390/ijms24043244

32. Tsuchida T, Lee YA, Fujiwara N, et al. A simple diet- and chemical-induced murine NASH model with rapid progression of steatohepatitis, fibrosis and liver cancer. *J Hepatol.* 2018;69(2):385-395. doi:10.1016/j.jhep.2018.03.011

33. Kumar DP, Caffrey R, Marioneaux J, et al. The PPAR α/γ Agonist Saroglitazar Improves Insulin Resistance and Steatohepatitis in a Diet Induced Animal Model of Nonalcoholic Fatty Liver Disease. Sci Rep. 2020;10(1):9330. Published 2020 Jun 9. doi:10.1038/s41598-020-66458-z

34. Poynard T, Munteanu M, Charlotte F, et al. Impact of steatosis and inflammation definitions on the performance of NASH tests. *Eur J Gastroenterol Hepatol*. 2018;30(4):384-391. doi:10.1097/MEG.0000000000001033

35. Brunt EM, Kleiner DE, Wilson LA, Sanyal AJ, Neuschwander-Tetri BA; Nonalcoholic Steatohepatitis Clinical Research Network. Improvements in Histologic Features and Diagnosis Associated With Improvement in Fibrosis in Nonalcoholic Steatohepatitis: Results From the Nonalcoholic Steatohepatitis Clinical Research Network Treatment Trials. *Hepatology.* 2019;70(2):522-531. doi:10.1002/hep.30418

36. Chatterjee B, Ghosh K, Kanade SR. Curcumin-mediated demethylation of the proximal promoter CpG island enhances the KLF4 recruitment that leads to increased expression of p21Cip1 in vitro. *J Cell Biochem.* 2019;120(1):809-820. doi:10.1002/jcb.27442

37. Kanai M, Wei D, Li Q, et al. Loss of Krüppel-like factor 4 expression contributes to Sp1 overexpression and human gastric cancer development and progression. *Clin Cancer Res*. 2006;12(21):6395-6402. doi:10.1158/1078-0432.CCR-06-1034

38. Hashemi M, Sabouni E, Rahmanian P, et al. Deciphering STAT3 signaling potential in hepatocellular carcinoma: tumorigenesis, treatment resistance, and pharmacological significance. *Cell Mol Biol Lett.* 2023;28(1):33. doi:10.1186/s11658-023-00438-9

39. Suresh D, Srinivas AN, Prashant A, Harikumar KB, Kumar DP. Therapeutic options in hepatocellular carcinoma: a comprehensive review [published online ahead of print, 2023 Feb 13]. *Clin Exp Med.* 2023;10.1007/s10238-023-01014-3. doi:10.1007/s10238-023-01014-3

40. Li Y, Martin RC 2nd. Herbal medicine and hepatocellular carcinoma: applications and challenges. *Evid Based Complement Alternat Med.* 2011;2011:541209. doi: 10.1093/ecam/neq044.

41. Choudhari AS, Mandave PC, Deshpande M, Ranjekar P, Prakash O. Phytochemicals in Cancer Treatment: From Preclinical Studies to Clinical Practice. *Front Pharmacol.* 2020;10:1614. doi:10.3389/fphar.2019.01614

42. Hamzawy MA, El-Denshary ESM, Abdel-Wahhab MA. Effects of natural compounds in treatment and prevention of hepatotoxicity and hepatocellular carcinoma. *Hepatoma Research.* 2015; 1:111-8. http://dx.doi.org/10.4103/2394-5079.167378

43. He Y, Yue Y, Zheng X, Zhang K, Chen S, Du Z. Curcumin, inflammation, and chronic diseases: how are they linked?. *Molecules*. 2015;20(5):9183-9213. doi:10.3390/molecules20059183

44. Pourbagher-Shahri AM, Farkhondeh T, Ashrafizadeh M, Talebi M, Samargahndian S. Curcumin and cardiovascular diseases: Focus on cellular targets and cascades. *Biomed Pharmacother.* 2021;136:111214. doi:10.1016/j.biopha.2020.111214

45. Bai C, Zhao J, Su J, et al. Curcumin induces mitochondrial apoptosis in human hepatoma cells through BCLAF1-mediated modulation of PI3K/AKT/GSK-3β signaling. *Life Sci.* 2022;306:120804. doi:10.1016/j.lfs.2022.120804

46. Pan Z, Zhuang J, Ji C, Cai Z, Liao W, Huang Z. Curcumin inhibits hepatocellular carcinoma growth by targeting VEGF expression. *Oncol Lett.* 2018;15(4):4821-4826. doi:10.3892/ol.2018.7988

47. Febbraio MA, Reibe S, Shalapour S, Ooi GJ, Watt MJ, Karin M. Preclinical Models for Studying NASH-Driven HCC: How Useful Are They?. *Cell Metab.* 2019;29(1):18-26. doi:10.1016/j.cmet.2018.10.012

48. Peiseler M, Tacke F. Inflammatory Mechanisms Underlying Nonalcoholic Steatohepatitis and the Transition to Hepatocellular Carcinoma. *Cancers (Basel).* 2021;13(4):730. doi:10.3390/cancers13040730

49. Barry AE, Baldeosingh R, Lamm R, et al. Hepatic Stellate Cells and Hepatocarcinogenesis. *Front Cell Dev Biol.* 2020;8:709. doi:10.3389/fcell.2020.00709

Figure Legends

Figure 1. Curcumin (CUR) treatment reduced obesity and improved liver injury and insulin resistance in WDSW/CCl_4 mice.
Mice were given either CDNW or WDSW for 12 weeks before being divided into two further groups and treated with either vehicle (VC) or curcumin (CUR) for the next 12 weeks (A). Before euthanasia, mice were measured for (B) body weight and (C) liver weight. Blood collected from overnight fasted mice was used for determining (D) ALT, (E) AST, and (F) total cholesterol. (G) Fasting glucose and (H) fasting insulin were measured, and (I) HOMA-IR was calculated using the formula (fasting insulin (milliunits/liter) - fasting glucose (mmol/liter))/22.5. All the data are expressed as mean±SEM with 6-8 mice in each group. ## $p < 0.001$ or # $p < 0.05$ compared to CDNW/CCl_4 with vehicle control; ** $p < 0.001$ or * $p < 0.05$ compared to WDSW/CCl_4 with vehicle control.

Figure 2. Curcumin (CU) treatment improves NASH and attenuates liver carcinogenesis. CDNW/CCl_4 or WDSW/CCl_4 mice were treated with vehicle (VC) or curcumin (CUR) for 12 weeks. (A) Representative images of the liver depicting the presence or absence of tumors, (B) Representative microscopic images of liver sections of each group stained with hematoxylin & eosin. Histology scores for (C) hepatic steatosis, (D) hepatocyte ballooning, (E) lobular inflammation, and (F) NAFLD activity score. (G) tumor numbers and (H) tumor histology. Data are expressed as mean±SEM with 6-8 mice in each group. ## $p < 0.001$ or # $p < 0.05$

compared to CDNW/CCl_4 with vehicle control; ** $p < 0.001$ or * $p < 0.05$ compared to WDSW/CCl_4 with vehicle control.

Figure 3. Curcumin (CU) treatment suppresses hepatic inflammation in NASH-HCC mice. The relative hepatic mRNA expression of (A) IL-1β, (B) IL-6, and (C) TNFα was determined by qRT-PCR. The expression levels were normalized with β-actin and carried out in triplicate. Immunoblots performed in the whole cell lysates of liver tissues treated with vehicle (VC) or curcumin (CUR) for (D) p-Erk1/2 and Erk1/2, (E) p-JNK and JNK. Data are expressed as mean±SEM. ## $p < 0.001$ or # $p < 0.05$ compared to CDNW/CCl_4 with vehicle control; ** $p < 0.001$ or * $p < 0.05$ compared to WDSW/CCl_4 with vehicle control. IL-1β, interleukin-1β; IL-6, interleukin-6; TNFα, tumor necrosis factor α; p-Erk1/2, phospho-extracellular signal-regulated protein kinase; p-JNK, phospho-c-Jun N-terminal kinase.

Figure 4. Curcumin (CUR) treatment ameliorates liver fibrosis in NASH-HCC mice. CDNW/CCl_4 and WDSW/CCl_4 mice were treated with vehicle (VC) or curcumin (CUR) for 12 weeks. (A) Representative microscopic images of Sirius red staining of liver sections from each group. (B) Quantification of the Sirius red positive area. Hepatic mRNA expression of (C) αSMA and (D) TGF-β were estimated. Liver sections were immune stained for the (E) Ki67 marker and (F) quantified for the positive area. Hepatic mRNA expression of (G) CD31 and (H) AFP was measured by qRT-PCR. Data are expressed as mean±SEM. ## $p < 0.001$ or # $p < 0.05$ compared to CDNW/CCl_4 with vehicle control; ** $p < 0.001$ or * $p < 0.05$ compared to WDSW/CCl_4 with vehicle control. αSMA, alpha Smooth Muscle Actin; TGF β, transforming growth factor β; CD31, cluster of differentiation 31; AFP, alpha fetoprotein.

Figure 5. Curcumin treatment downregulates AATF expression. Liver tissues from vehicle control (VC) and curcumin (CUR) treated mice from CDNW/CCl_4 and WDSW/CCl_4 were processed. (A) Representative micrographs of AATF immunostaining in all four groups. (B) Relative mRNA expression of AATF in mouse liver tissues normalized to the endogenous control, β-actin. Viability of QGY-7703 cells following curcumin treatment with different concentrations (C) and time (D). The mRNA expression (E) and immunoblot (F) of AATF in control and AATF knockdown (KD) QGY-7703 cells treated with vehicle (VC) or curcumin (CUR). (G) Cell viability of control and AATF knockdown (KD) QGY-7703 cells treated with vehicle (VC or curcumin (CUR) normalized against control. (H) Representative micrographs (100X) and quantification of cell migration of control and AATF knockdown (KD) QGY-7703 cells treated with vehicle (VC) or curcumin (CU). Data are expressed as mean±SEM. ## $p < 0.001$ or # $p < 0.05$ compared to CDNW/CCl_4 with vehicle control; ** $p < 0.001$ or * $p < 0.05$ compared to WDSW/CCl_4 with vehicle control or AATF control cells treated with vehicle.

Figure 6. Curcumin downregulates AATF via KLF4 and Sp1 signaling pathway. The relative mRNA expression of KLF4 (A) and Sp1 (B) and (C) immunoblots of KLF4 and Sp1 normalized to the endogenous control β-actin from CDNW/CCl_4 and WDSW/CCl_4 mice treated with vehicle (VC) or curcumin (CUR). QGY-7703 cells treated with vehicle (VC) or curcumin (CUR) were examined for the mRNA and

protein expression of KLF4 (D and E) and Sp1 (F and G). Whole cell lysates prepared from the control and AATF knockdown (KD) QGY-7703 cells treated with vehicle (VC) or curcumin (CUR) were also checked for the expression of pSTAT3 and STAT3, pSTAT3 normalized to its control STAT3. Data are expressed as mean±SEM. ** $p < 0.001$ or * $p < 0.05$ compared to WDSW/CCl_4 with vehicle control or AATF control cells treated with vehicle. KLF4, kruppel-like factor 4; Sp1, specificity protein 1.

Figure 7. Schematic representation of the molecular mechanisms involved in curcumin-mediated amelioration of NASH-HCC via AATF. CDNW/CCl_4 and WDSW/CCl_4 were treated with curcumin for 12 weeks. Administration of curcumin ameliorated steatohepatitis (NASH), fibrosis and progression to HCC in WDSW/CCl_4 mice by downregulating AATF expression via KLF4 and Sp1 signaling pathway.

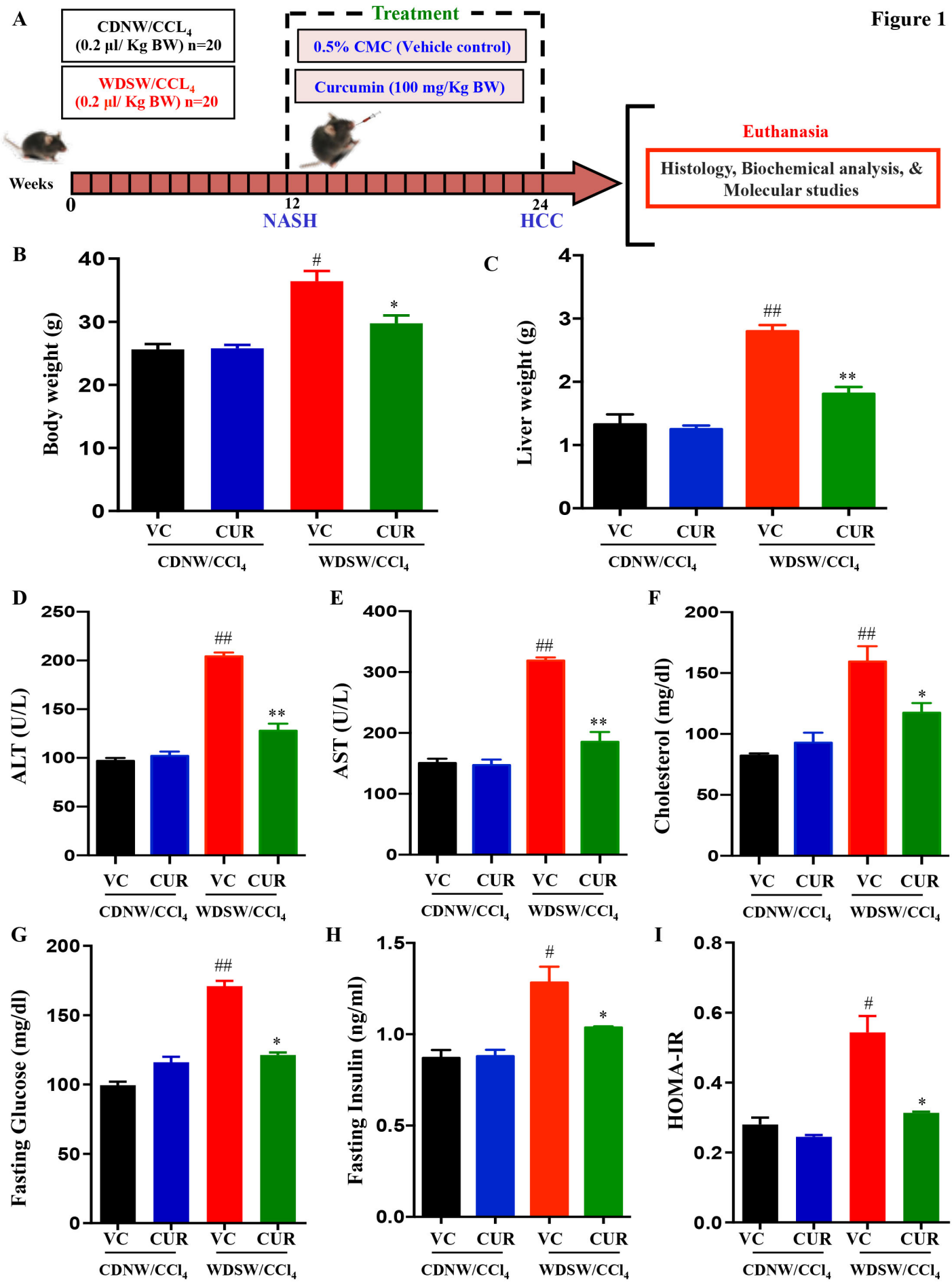
Figure 1
A
CDNW/CCL4 (0.2 µl/ Kg BW) n=20
WDSW/CCL4 (0.2 µl/ Kg BW) n=20
Treatment
0.5% CMC (Vehicle control)
Curcumin (100 mg/Kg BW)
Weeks
0
12
24
NASH
HCC
Euthanasia
Histology, Biochemical analysis, & Molecular studies
B
Body weight (g)
C
Liver weight (g)
D
ALT (U/L)
E
AST (U/L)
F
Cholesterol (mg/dl)
G
Fasting Glucose (mg/dl)
H
Fasting Insulin (ng/ml)
I
HOMA-IR
VC
CUR
CDNW/CCl4
WDSW/CCl4

Figure 2

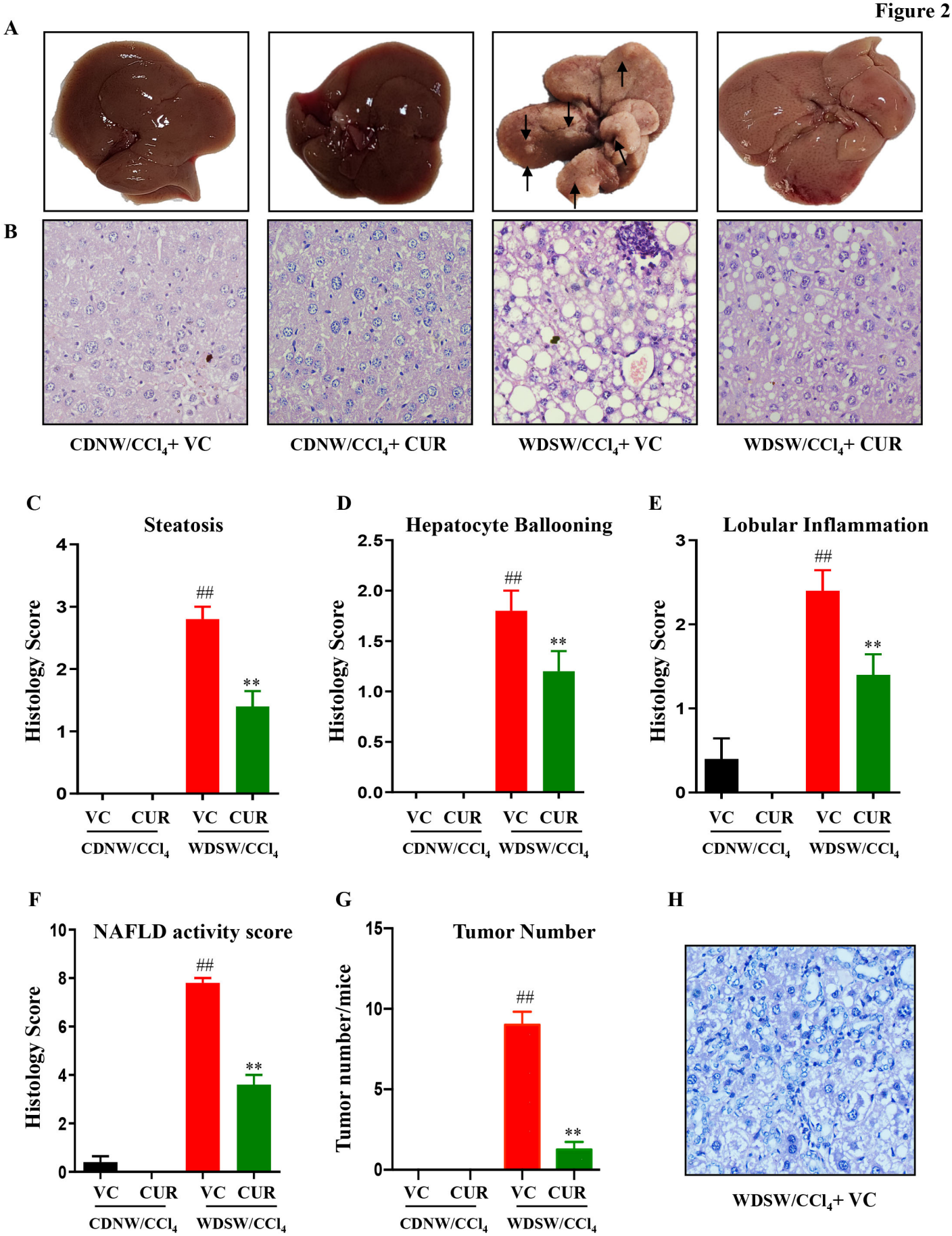
A
B
CDNW/CCl4+ VC
CDNW/CCl4+ CUR
WDSW/CCl4+ VC
WDSW/CCl4+ CUR
C
Steatosis
Histology Score
D
Hepatocyte Ballooning
Histology Score
E
Lobular Inflammation
Histology Score
F
NAFLD activity score
Histology Score
G
Tumor Number
Tumor number/mice
H
WDSW/CCl4+ VC
VC CUR VC CUR
CDNW/CCl4 WDSW/CCl4
##
**

Figure 3

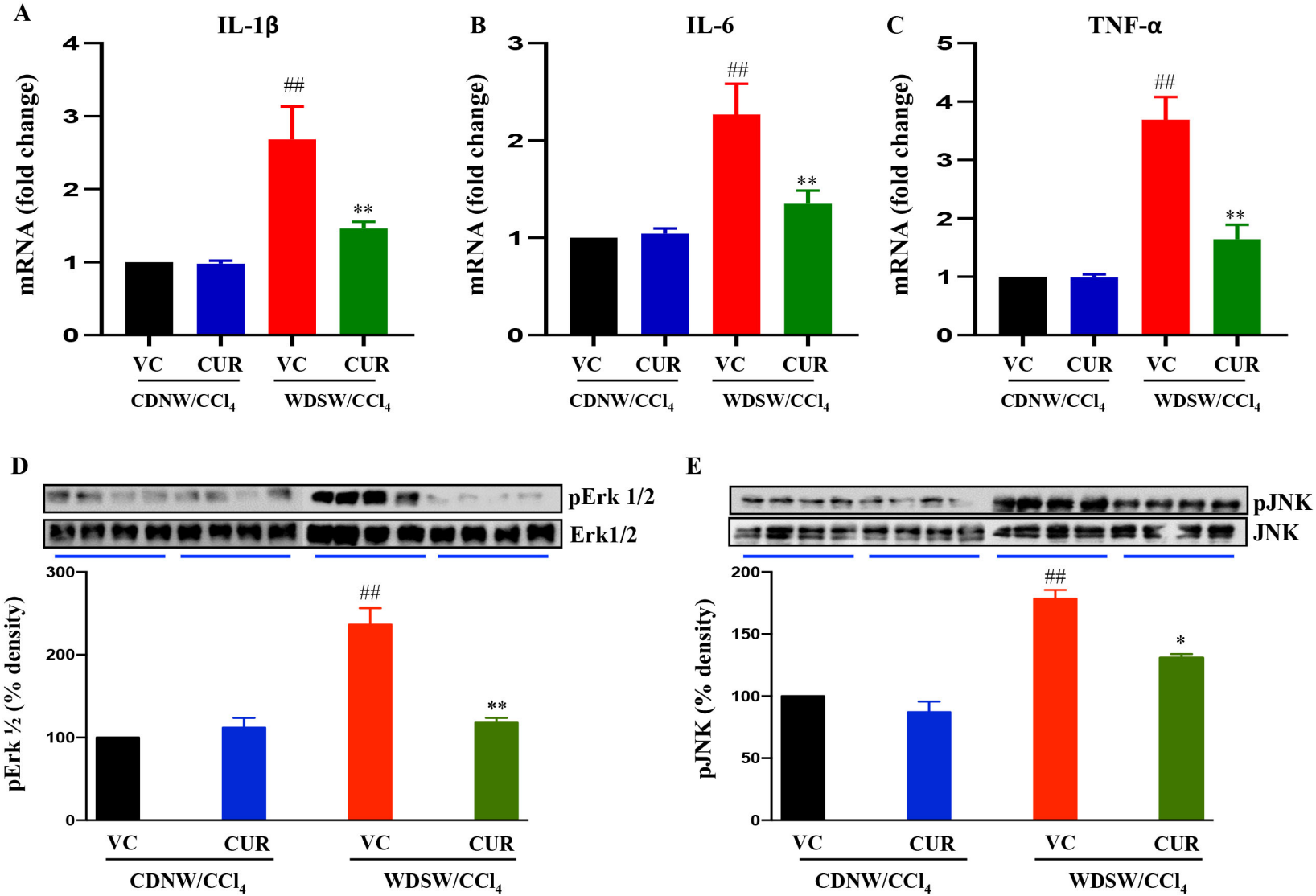
A
IL-1β
mRNA (fold change)
0
1
2
3
4
##
**
VC
CUR
VC
CUR
CDNW/CCl4
WDSW/CCl4
B
IL-6
mRNA (fold change)
0
1
2
3
##
**
VC
CUR
VC
CUR
CDNW/CCl4
WDSW/CCl4
C
TNF-α
mRNA (fold change)
0
1
2
3
4
5
##
**
VC
CUR
VC
CUR
CDNW/CCl4
WDSW/CCl4
D
pErk 1/2
Erk1/2
pErk ½ (% density)
0
100
200
300
##
**
VC
CUR
VC
CUR
CDNW/CCl4
WDSW/CCl4
E
pJNK
JNK
pJNK (% density)
0
50
100
150
200
##
*
VC
CUR
VC
CUR
CDNW/CCl4
WDSW/CCl4

Figure 4

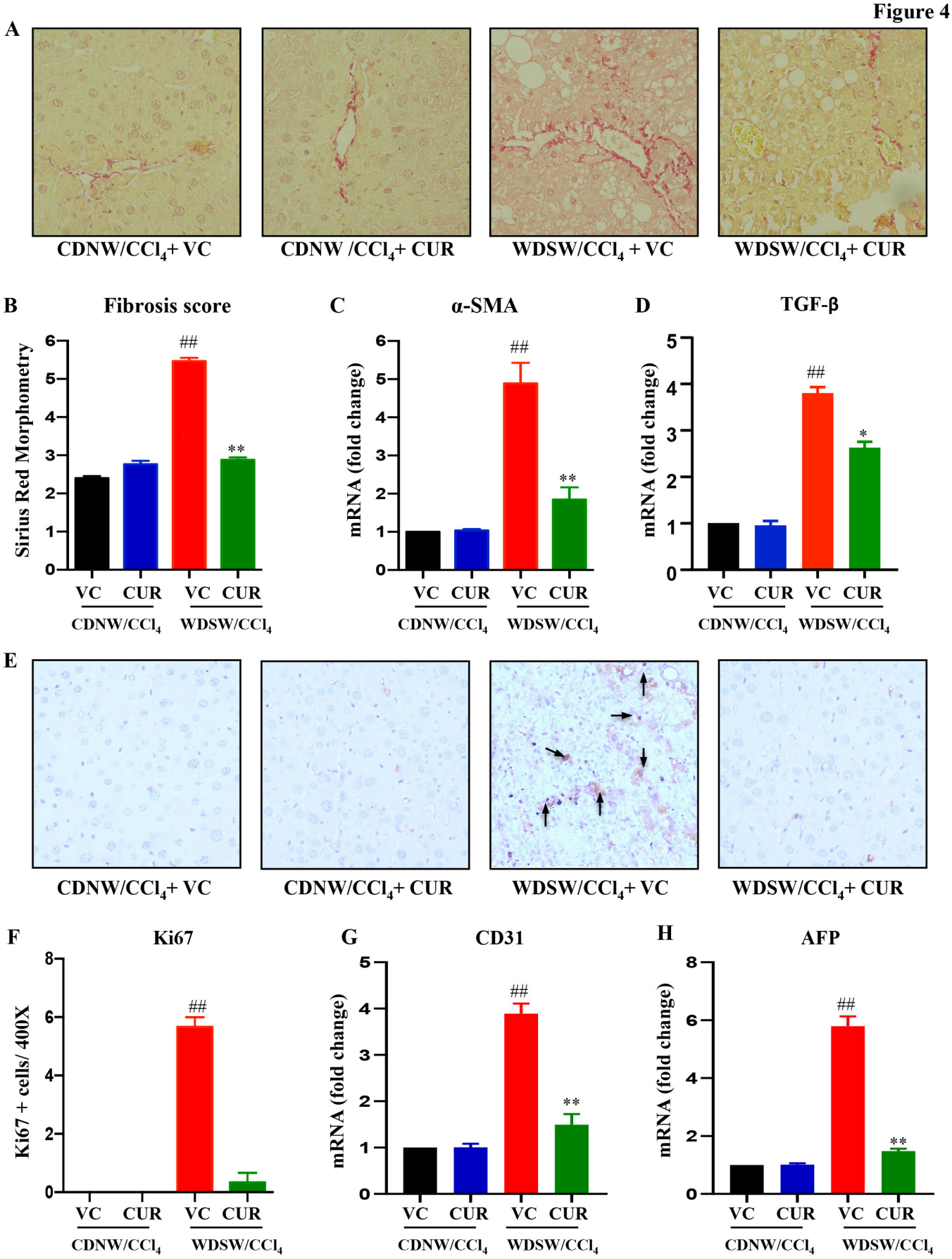
A
CDNW/CCl4+ VC
CDNW /CCl4+ CUR
WDSW/CCl4 + VC
WDSW/CCl4+ CUR
B
Fibrosis score
Sirius Red Morphometry
C
α-SMA
mRNA (fold change)
D
TGF-β
mRNA (fold change)
VC CUR VC CUR
CDNW/CCl4 WDSW/CCl4
##
**
*
E
CDNW/CCl4+ VC
CDNW/CCl4+ CUR
WDSW/CCl4+ VC
WDSW/CCl4+ CUR
F
Ki67
Ki67 + cells/ 400X
G
CD31
mRNA (fold change)
H
AFP
mRNA (fold change)

Figure 5

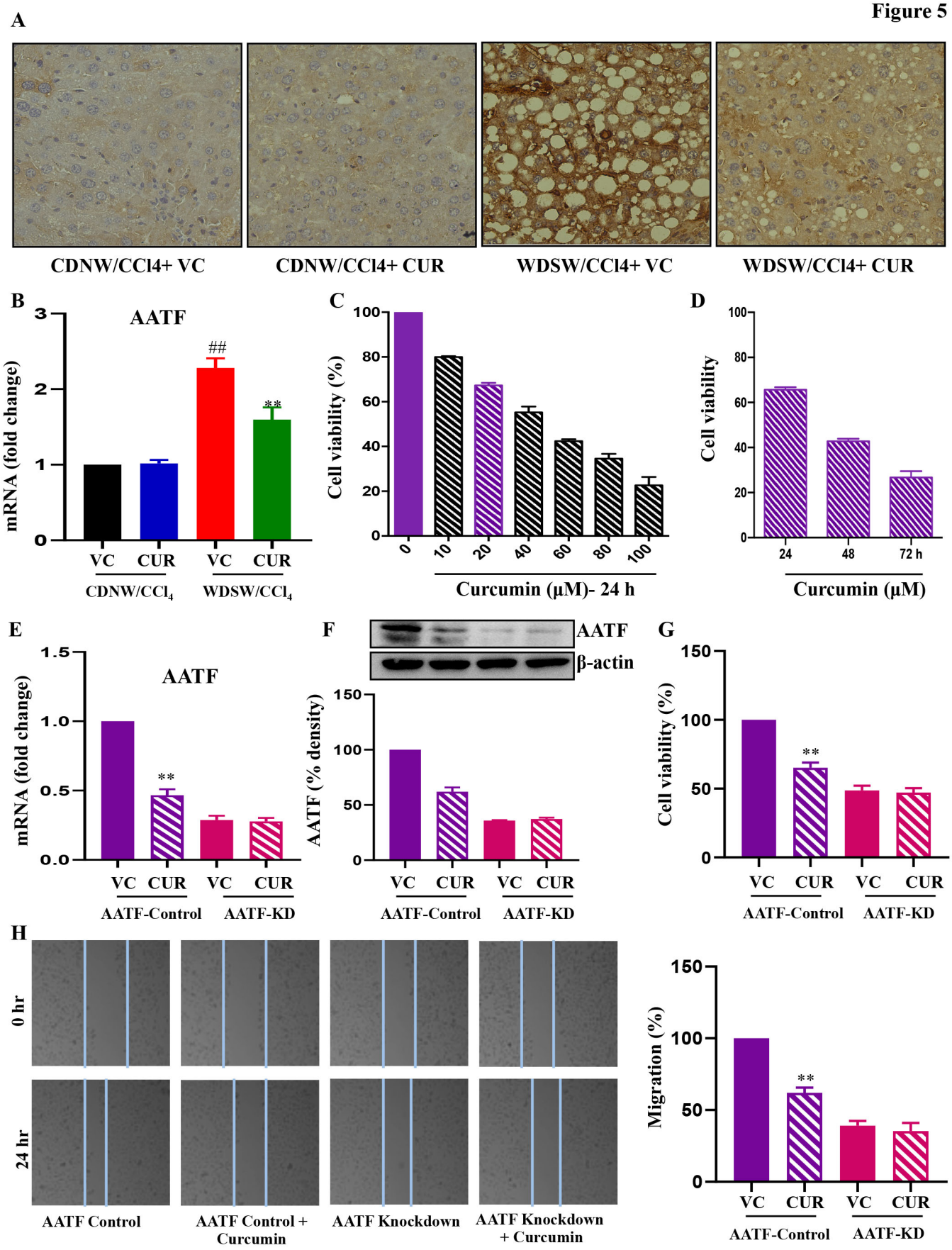
A
CDNW/CCl4+ VC
CDNW/CCl4+ CUR
WDSW/CCl4+ VC
WDSW/CCl4+ CUR
B
AATF
mRNA (fold change)
##
**
VC CUR VC CUR
CDNW/CCl4
WDSW/CCl4
C
Cell viability (%)
Curcumin (μM)- 24 h
D
Cell viability
24 48 72 h
Curcumin (μM)
E
AATF
mRNA (fold change)
**
VC CUR VC CUR
AATF-Control AATF-KD
F
AATF
β-actin
AATF (% density)
VC CUR VC CUR
AATF-Control AATF-KD
G
Cell viability (%)
**
VC CUR VC CUR
AATF-Control AATF-KD
H
0 hr
24 hr
AATF Control
AATF Control + Curcumin
AATF Knockdown
AATF Knockdown + Curcumin
Migration (%)
**
VC CUR VC CUR
AATF-Control AATF-KD

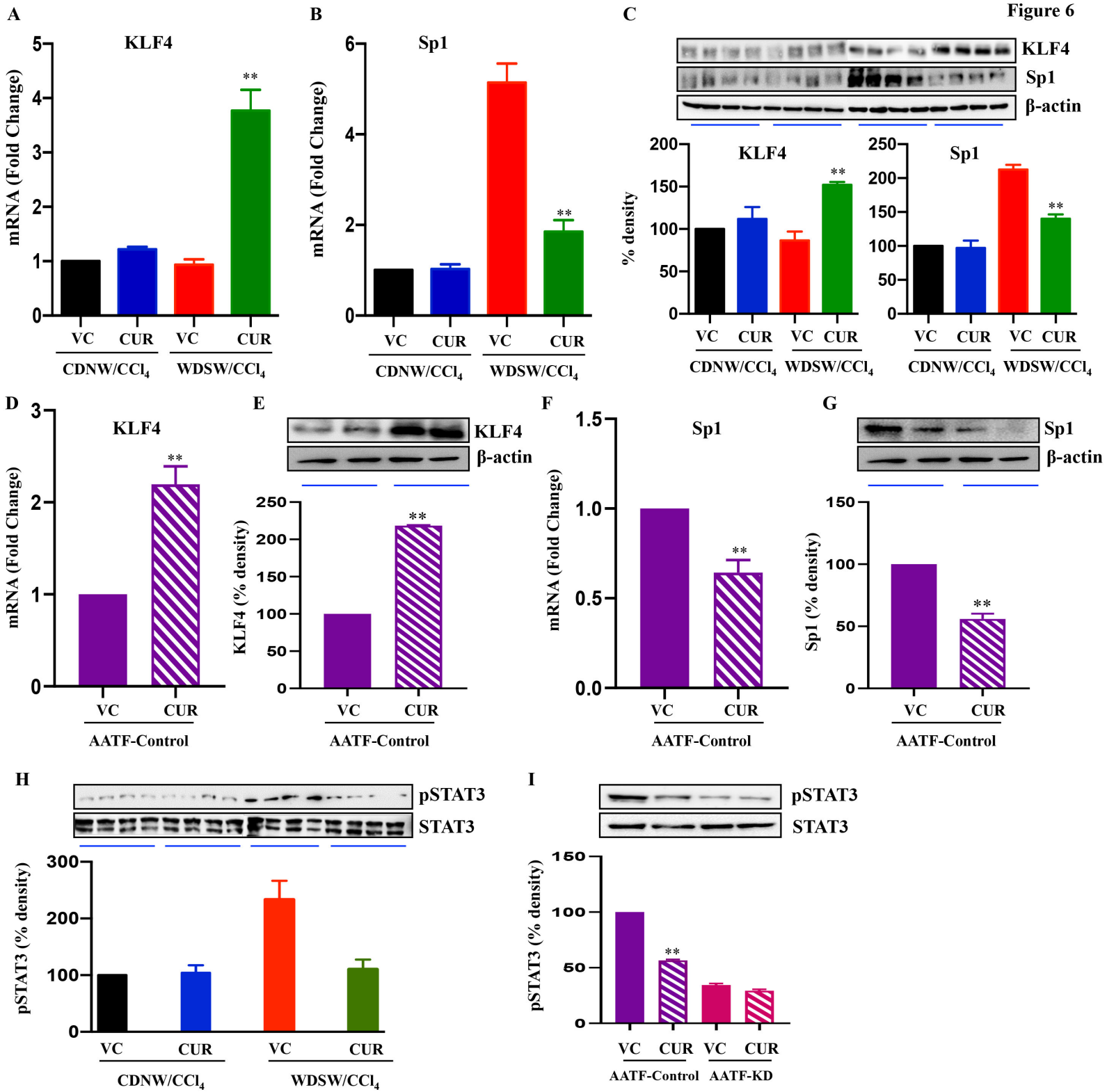
Figure 6
A
KLF4
mRNA (Fold Change)
VC
CUR
VC
CUR
CDNW/CCl4
WDSW/CCl4
B
Sp1
mRNA (Fold Change)
C
KLF4
Sp1
β-actin
% density
D
KLF4
mRNA (Fold Change)
AATF-Control
E
KLF4
β-actin
KLF4 (% density)
F
Sp1
mRNA (Fold Change)
G
Sp1
β-actin
Sp1 (% density)
H
pSTAT3
STAT3
pSTAT3 (% density)
I
pSTAT3
STAT3
pSTAT3 (% density)
AATF-KD

Figure 7

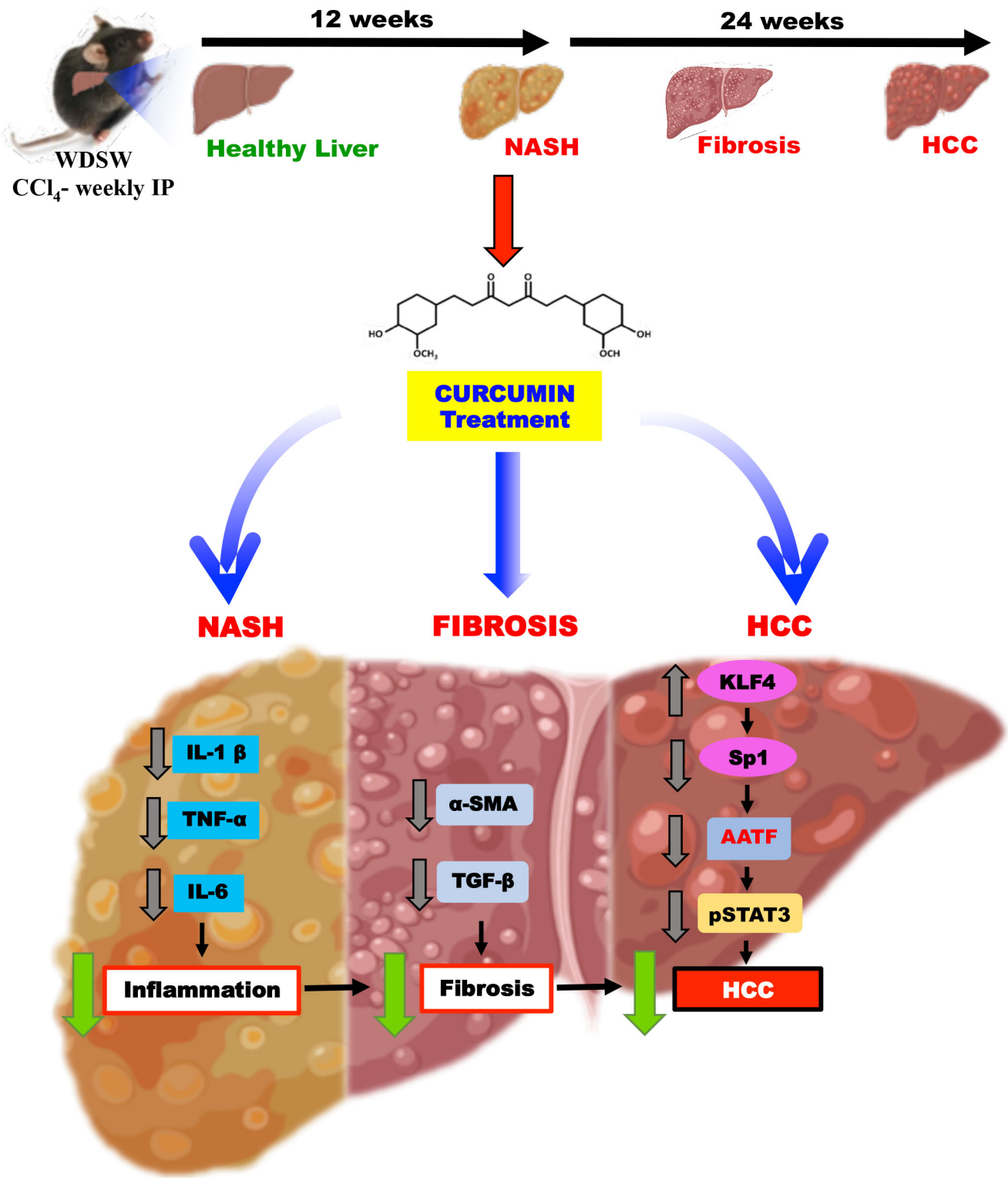
12 weeks
24 weeks
WDSW
CCl4- weekly IP
Healthy Liver
NASH
Fibrosis
HCC
CURCUMIN Treatment
NASH
FIBROSIS
HCC
IL-1 β
TNF-α
IL-6
Inflammation
α-SMA
TGF-β
Fibrosis
KLF4
Sp1
AATF
pSTAT3
HCC